Published in final edited form as:
Nat Immunol. 2010 May ; 11(5): 411–418. doi:10.1038/ni.1857.

Toll-like receptor activation of XBP1 regulates innate immune responses in macrophages

Fabio Martinon[1], **Xi Chen**[1], **Ann-Hwee Lee**[1,2], and **Laurie H. Glimcher**[1,2,3]

[1]Dept. of Immunology and Infectious Diseases, Harvard School of Public Health, 651 Huntington Ave, Boston, MA 02115, USA

[2]Dept of Medicine, MIT and Harvard, Harvard Medical School, 651 Huntington Ave, Boston, MA 02115, USA

[3]Ragon Institute of MGH, MIT and Harvard, Harvard Medical School, 651 Huntington Ave, Boston, MA 02115, USA

Abstract

Sensors of pathogens, such as Toll-like receptors (TLRs), detect microbes to activate transcriptional programs that orchestrate adaptive responses to specific insults. Here we report that TLR4 and TLR2 specifically activated the endoplasmic reticulum (ER)-stress sensor kinase IRE1α and its downstream target, the transcription factor XBP1. Previously described XBP1 ER stress target genes were not induced by TLR signaling. Instead, TLR-activated XBP1 was required for optimal and sustained production of proinflammatory cytokines in macrophages. Consistent with this finding, IRE1α activation by ER-stress synergized with TLR activation for cytokine production. Moreover, XBP1 deficiency markedly increased bacterial burden in animals infected with the TLR2-activating human pathogen *Francisella tularensis*. Our findings uncover an unsuspected critical new function for the XBP1 transcription factor in mammalian host defenses.

Keywords

ER-stress; IRE1; XBP1; TLR; innate immunity

The innate immune system recognizes key molecular signatures of pathogens or pathogen-associated molecular patterns (PAMPs) that include structural components like lipopolysaccharide (LPS) and peptidoglycans (PGN), as well as double-stranded (ds) RNA and DNA. PAMP recognition by the host organism occurs through a group of receptors referred to as pathogen recognition receptors (PRRs), the best studied being the Toll-like receptors (TLRs)[1]. The cytoplasmic domains of TLRs contain a Toll–IL-1R homology (TIR) domain that forms a platform for downstream signaling by recruiting TIR domain-containing adapters including MyD88 [http://www.signaling-gateway.org/molecule/query?afcsid=A003535], TIR domain-containing adaptor (TIRAP), and TIR domain-containing adaptor inducing interferon-β (TRIF)[2, 3]. Engagement of TLR proximal signaling complexes leads to a sequential cascade

Correspondence should be addressed to Laurie H. Glimcher, Department of Immunology and Infectious Diseases, FXB Building, Room 205, 651 Huntington Avenue, Boston, MA 02115, Phone: 617-432-0622, lglimche@hsph.harvard.edu.

Authors Contributions

F.M. and L.H.G designed the research; F.M. and X.C. performed the experiments; A.-H. L. contributed critical reagents; F.M., X.C., A.-H. L. and L.H.G analyzed the results; F.M. and X.C. made the figures; F.M. and L.H.G wrote the paper.

Supporting Online Material: Supplementary Fig.1-9

of transcriptional regulatory events that vary depending on the TLR agonists, cell types involved and pathogenicity of the microbe. Individual genes (notably those encoding proinflammatory cytokines) are induced transiently and then repressed, reflecting the ability that the innate immune system has to interpret the infection and orchestrate appropriate responses while promoting resolution[4-6]. Microbial products are not the only signals that modulate innate immune responses, signals produced by stressed or damaged tissues have also been suggested to modulate the inflammatory response[7-9].

The endoplasmic reticulum (ER)-stress response identifies a group of signals that cope with perturbations in ER homeostasis. This adaptive response activates two parallel kinases (IRE1 [http://www.signaling-gateway.org/molecule/query?afcsid=A003134] and PERK) and a transcription factor precursor (ATF6), that instigate distinct signaling pathways[10]. The most conserved signaling branch consists of IRE1, an ER-anchored kinase that functions by activating the transcription factor XBP1. The XBP1 mRNA encodes for a non-functional protein that is activated via an IRE1-dependent unconventional cytosolic mRNA splicing event that generates a mature XBP1 protein (XBP1s) harboring a potent transactivation domain. Although all three branches are activated simultaneously, the responses set in motion via IRE1 are rapidly attenuated despite the persistence of stress, while those downstream of PERK activation are sustained. This observation has led to the suggestion that IRE1 and XBP1 function to facilitate homeostasis in the adaptation phase of the response while PERK activation may favor cell death via its downstream transcription factor CHOP[11].

Large-scale gene expression studies have reported transcriptional induction of the *XBP1* mRNA precursor upon TLR stimulation[5] and upon infection of human macrophages or mouse lung tissues with pathogenic *Mycobacteria* and *Klebsiella pneumoniae* species[12-14]. Although these studies did not investigate XBP1 mRNA maturation, they demonstrate that the IRE1 substrate is produced upon TLR stimulation. Some ER-stress markers were also detected upon sustained LPS stimulation[15-17]. In the liver, for example, the ER-stress response has been shown to promote inflammation by upregulating expression of acute phase proteins[17]. Altogether these observations prompted us to investigate a possible link between ER-signaling and innate immunity.

Here we identify a novel function of the XBP1 branch of the ER-stress pathway, as a positive regulator of TLRs responses in macrophages. We show that TLRs engaged IRE1α to promote cytosolic splicing and activation of the XBP1 transcription factor. Activation of IRE1α and XBP1 by TLRs occurred in the absence of an ER-stress response and did not contribute to the induction of ER-stress induced genes. Instead, IRE1 activation of XBP1 was required to promote sustained production of inflammatory mediators, including interleukin 6 (IL-6), demonstrating that a specific branch of the ER-stress response can operate independently of the other branches. Consistent with a positive function of XBP1 in TLR responses, increased production of active XBP1 by pharmacologically ER-stressed macrophages exacerbated TLR responses. Moreover, XBP1-deficient mice infected with *F. tularensis* live vaccine strain (LVS) had increased bacterial burden and reduced production of inflammatory mediators.

RESULTS

TLRs trigger XBP1 activation in macrophages

We tested whether TLRs might activate the ER stress response. We stimulated mouse J774 macrophages with the TLR4 agonist LPS and analyzed IRE1α, PERK and ATF6α activation. We measured ATF6α activation by monitoring the liberation of its cleaved fragment and PERK and IRE1α activation by examining their phosphorylation status. To

detect active IRE1α, we used the Phos-tag reagent that selectively binds to phosphorylated amino acid residues[18,19]. In polyacrylamide gels containing Phos-tag acrylamide, phosphorylated forms of IRE1α could be detected by slower migration upon stimulation with LPS. However, neither ATF6α nor PERK activation was detected (Fig. 1a). To further examine the effects of TLR signaling on the classical ER stress response, we stimulated cells with tunicamycin (TM), a potent pharmacologic ER-stress inducer, in the presence or absence of LPS or Pam_3CSK_4, a TLR2 agonist. TM alone induced activation of the ER stress response as expected. Despite IRE1α activation, we found that LPS or Pam_3CSK_4 did not induce a classic ER-stress response[10] as measured by CHOP, BiP, ERdj4 and PDI expression. In fact, LPS or Pam_3CSK_4 co-treatment repressed the ER-stress-induced mRNAs including CHOP, PDI and ERdj4 and the proteolytic processing of ATF6α triggered by TM treatment of J774 macrophages (Fig. 1b and Supplementary Fig.1a). Similar to the results obtained in co-stimulation experiments, pre-stimulation of macrophages with TLR agonists substantially inhibited TM-mediated PERK and ATF6 activation as well as CHOP or PDI mRNA production (Supplementary Fig.1b,c). Moreover, short-term stimulation with LPS or Pam_3CSK_4 inhibited ER-stress induced genes in macrophages pretreated with TM (Supplementary Fig.1d). Interestingly, TM mediated recruitment of XBP1s to the *Dnajb9* promoter (encoding ERdj4) was reduced in the presence of LPS, further demonstrating that TLR4 signaling blocks ER-stress responses (Supplementary Fig.1e). By analyzing primary macrophages from MyD88-deficient mice, we observed that TLR2 (Pam_3CSK_4) dampening of the ER-stress response was MyD88 dependent, while TLR4 dampening was only partially dependent on MyD88 (Supplementary Fig.1f). We conclude that TLR2 and TLR4 trigger IRE1α activation while inhibiting the ER-stress response.

Since TLR signaling did not induce the expression of known XBP1 target genes, we asked whether TLRs activate XBP1 mRNA splicing. IRE1α-mediated splicing of XBP1 mRNA generates XBP1s, a potent transcriptional activator. Splicing of XBP1 mRNA and production of XBP1s protein was detected as early as 3 h after LPS stimulation (Fig. 1c). As above, CHOP and ATF6α, two transcription factors that are induced or activated upon ER-stress were not detected following TLR stimulation. Interrogation of a panel of TLR agonists revealed that agonists engaging TLR2, TLR4 and TLR5 but not TLR3, TLR7 or TLR9 promoted XBP1 splicing (Fig. 1d). XBP1s production upon TLR4 and TLR2 stimulation was IRE1α dependent as demonstrated by defective LPS- or Pam_3CSK_4-induced XBP1 mRNA splicing in cells treated with IRE1α-specific short-hairpin RNAs (shRNAs) (Fig. 1e). TLR activation of XBP1 was also observed in primary macrophages from wild-type mice (C3H/HeOuJ) upon LPS stimulation. Macrophages isolated from mice carrying a mutation in the signaling domain of TLR4 (C3H/HeJ) did not activate XBP1 upon LPS stimulation (Fig. 1f). Similarly, the TLR2 agonists Pam_3CSK_4 and FSL1 did not activate XBP1 splicing in TLR2-deficient macrophages (Supplementary Fig. 2), demonstrating that XBP1 splicing was triggered by TLRs rather than by a potential direct effect of these PAMPs on the ER.

TLR activation of XBP1 is TRAF6 and NOX2 dependent

To identify the downstream effectors of TLRs that mediate XBP1 activation, we interrogated XBP1 splicing in macrophages from mice deficient for the TIR adaptors MyD88, TRIF or TIRAP. TLR2 induced splicing of XBP1 was dependent on the TIRAP-MyD88 signaling pathway, while TRIF or MyD88 deficiency only partially inhibited TLR4 activation of XBP1, suggesting that both MyD88-dependent and MyD88-independent (TRIF-dependent) signaling lead to TLR4-induced XBP1 splicing (Fig. 2a). Both TRIF and MyD88 are known to engage the signaling molecule TRAF6 [http://www.signaling-gateway.org/molecule/query?afcsid=A002312] and the downstream

NF-κB scaffolding protein NEMO[2]. Analysis of J774 macrophage populations stably expressing shRNAs targeting TRAF6 or NEMO revealed that TRAF6 was required for XBP1 splicing mediated by TLR2 and TLR4; in contrast, NEMO was dispensable (Fig. 2b). As control, both NEMO and TRAF6 knockdown populations failed to induce *Il6* transcription upon LPS stimulation (Fig. 2b) and did not affect TM-mediated XBP1 mRNA activation (Supplementary Fig. 3a). Further, pharmacological inhibition of NF-κB, p38, c-Jun N-terminal kinase (JNK) and mitogen-activated protein kinase kinase (MEK) pathways did not affect LPS-induced XBP1 splicing (Supplementary Fig. 3b) confirming that splicing is mediated by TRAF6 activation independently of NF-κB, p38 and JNK pathways.

TRAF proteins can bind and activate nicotinamide adenine dinucleotide phosphate (NADPH)-oxidase, a membrane-bound enzyme complex found in the plasma membrane as well as in phagosome membranes[20-22]. The NADPH-oxidase NOX2 [http://www.signaling-gateway.org/molecule/query?afcsid=A002484] mediates the induction of reactive oxygen species (ROS) by TLRs in macrophages[23]. Use of NADPH oxidase inhibitors diphenyleneiodonium chloride (DPI) and apocynin, or NOX2 deficiency abolished XBP1 splicing by LPS or Pam_3CSK_4, but not by TM treatment (Fig. 2c,d), demonstrating that TLR4 and TLR2 mediate XBP1 splicing by activating the NADPH-oxidase complex. Interestingly, oxidative stress has been previously shown to promote ER-stress[24], however pre-treatment with chemical chaperones that alleviate mild ER-stress, did not affect XBP1 activation further (Supplementary Fig. 3c). These data suggest that TLRs and NOX2 engage a specific IRE1-activating pathway.

TLR activation of XBP1 regulates cytokine production

To establish the function of XBP1 in TLR signaling, we used *Xbp1*$^{flox/flox–MxCre}$ mice (hereafter called XBP1$^{\Delta}$) lacking XBP1 in macrophages and other hematopoietic lineage cells[25]. Consistent with the results above, no induction of classic ER-stress related genes such as CHOP or PDI was observed upon stimulation of XBP1$^{\Delta}$ macrophages or wild-type macrophages with LPS. As control, TM induction of PDI and WSF1 was reduced in XBP1$^{\Delta}$ macrophages, indicating efficient XBP1 deletion (Supplementary Fig. 4). However, XBP1$^{\Delta}$ macrophages stimulated with TLR4 or TLR2 agonists displayed impaired secretion of IL-6 as measured by ELISA (Fig. 3a) and impaired production of other inflammatory mediators including tumor necrosis factor (TNF), interferon-β (IFN-β), the ubiquitin-like modifier ISG15 and cyclooxygenase 2 (COX2) in addition to IL-6 as measured by quantitative RT-PCR (Fig. 3b). The defect was specific to certain mediators since other cytokines such as IL-1β and RANTES were unaffected by XBP1 deficiency (Fig. 3b). Interestingly, XBP1$^{\Delta}$ macrophages did not display an absolute defect, rather we found that early (1 h) IL-6 mRNA induction was comparable to wild-type but that IL-6 mRNA production was defective at later (6 h) time points (Fig. 3c). Consistent with the unperturbed early cytokine profile, early induction of IκBβ degradation, JNK phosphorylation and macrophage viability were not affected (Supplementary Fig. 5a). Taken together, these findings demonstrate that XBP1 in macrophages is required downstream of TLR2 and TLR4 for sustained production of innate immune mediators such as IL-6.

XBP1 activation by ER stress enhances TLR signaling

The experiments above suggested that activation of the IRE1-XBP1 signaling pathway by the innate immune system in macrophages is required for optimal secretion of certain proinflammatory cytokines. We asked whether augmenting this pathway through pharmacologic induction of an ER stress response would enhance the natural response to microbial products. Indeed, LPS treatment increased TM-induced XBP1 splicing but not in TLR4-unresponsive macrophages (Fig. 1f, compare increased splicing in lanes 6 and 7 in C3H/HeOuJ macrophages with no change in splicing in C3H/HeJ macrophages).

Remarkably, the amounts of IL-6 and ISG15 produced by LPS-stimulated macrophages were synergistically increased when the cells were simultaneously ER-stressed with TM (Fig. 4a). To demonstrate that this effect was triggered by IRE1α, we transduced J774 macrophages with a constitutively active recombinant protein encoding the cytosolic kinase and ribonuclease domain of IRE1α[26]. A marked augmentation of IL-6 production was observed in the presence of active IRE1α and LPS (Fig. 4b). Similarly, knockdown of BI-1, an ER-localized negative regulator of IRE1α[26], mediated an increased XBP1 activation and increased IL-6 production upon LPS treatment (Supplementary Fig. 6). As confirmation, knockdown of IRE1α in J774 macrophages resulted in reduced IL-6 induction by TM and LPS co-treatment (Fig. 4c). Importantly, this finding was confirmed in primary wild-type and XBP1$^{\Delta}$ macrophages that were left untreated or pre-treated for 12 h with a low dose of TM and then stimulated with LPS for 3 h. Wild-type but not XBP1$^{\Delta}$ macrophages displayed augmented IL-6 production (Fig. 4d). We also examined whether this newly identified pathway of XBP1 activation by TLRs alone and in concert with ER stressors was operative in human cells. Primary human macrophages infected with the intracellular pathogen *F. tularensis* LVS strain exhibited increased XBP1 splicing and a synergistic increase in cytokine production with addition of TM. Specifically, production of IL-6, TNF and IL-8 upon *F. tularensis* infection was considerably enhanced in the presence of TM (Fig. 4e).

We asked whether some or all genes encoding these cytokines may be direct XBP1 targets. ChIP experiments revealed substantial recruitment of XBP1 to the promoters of some inflammatory mediators including *Il6* and *Tnf*, but not *Il1b or Ccl5*, which encodes RANTES (Fig. 5a,b and Supplementary Fig. 7). These data suggest that XBP1 may contribute directly to the transcription of at least some of these inflammatory cytokines.

XBP1 is required for immune responses to *F.tularensis*

To test the function of this pathway in the handling of pathogens *in vitro*, we infected wild-type primary macrophages with three different pathogens that are agonists for TLR2 and/or TLR4, *Mycobacterium tuberculosis, Listeria monocytogenes* and *F. tularensis*. Infection with any of these three pathogens induced XBP1 spliced mRNA (Fig. 6a). We next investigated the physiologic relevance of these observations in the context of infection with the intracellular pathogen *F. tularensis*. The immune response to this intracellular bacterium and potential bioterrorism agent that causes the human disease tularemia has been studied in mice using the LVS strain[27]. Optimal immunity against *F. tularensis* requires TLR2 (refs. [28-30]) and cytokine secretion, including TNF, in macrophages[31]. Consistent with the observation that TLR2 is the main TLR activated by *F. tularensis*, we found that *F. tularensis* mediated XBP1 splicing was deficient in *Tlr2*$^{-/-}$ macrophages (Fig. 6b). Similarly, NOX2 deficiency impaired XBP1 activation upon infection with *F. tularensis* (Fig. 6b). We infected bone marrow-derived macrophages (BMMs) from *Tlr2*$^{-/-}$, *Cybb*$^{-/-}$ (which encode NOX2), XBP1$^{\Delta}$ and wild-type mice with the *F. tularensis* LVS strain and monitored production of inflammatory mediators by real-time PCR. TLR2 deficiency severely impaired cytokine production by *F. tularensis*, while optimum induction of IL-6 and TNF was NOX2 and XBP1-dependent (Fig. 6c and Supplementary Fig. 8a). In contrast, increased production of IL-1β was XBP1 and NOX2-independent (Fig. 6c).

To confirm that XBP1 potentiates *F. tularensis*-mediated cytokine production, we infected BMM from XBP1$^{\Delta}$ and wild-type mice in the presence or absence of TM. Consistent with the data using TLR agonists (Fig. 3d), we found that XBP1 was required for maximal synergistic induction of IL-6 in infected macrophages (Fig. 6d). TLR2 deficiency has been shown to result in decreased IL-6 and TNF production *in vivo* and increased bacterial load in *F. tularensis* infected mice[32, 33]. To test whether loss of XBP1 impairs the immune response to *F. tularensis in vivo*, we infected wild-type and XBP1$^{\Delta}$ mice with low doses of *F. tularensis* by aerosol exposure, a mimic of the often lethal human disease, pneumonic

tularemia. Survival of neither XBP1$^{\Delta}$ nor wild-type mice was significantly impaired. However, similar to TLR2-deficient mice, quantification of bacterial burden in various organs 7 days after aerosol infection revealed that bacterial burden was greater than one log higher in the spleen, lung and liver of XBP1$^{\Delta}$ mice compared with wild-type littermates (Fig. 6e). By day 14, both wild-type and XBP1$^{\Delta}$ BALB/c mice had cleared the infection as determined by the absence of bacteria in the spleen and liver although XBP1$^{\Delta}$ lungs harbored significantly greater bacterial loads than wild-type lungs even at day 14 (Fig. 6f). Consistent with the increased bacterial burden, histopathology of XBP1$^{\Delta}$ liver showed an increase in non-discrete neutrophil-rich granulomatous lesions compared with wild-type liver at day 7 postinfection (Supplementary Fig. 8b). Hence, XBP1 is involved in the early protective host innate immune response to infection with *F. tularensis* but likely is not important in the adaptive immune response to this organism. This finding is consistent with our unpublished observations that XBP1 splicing is not evident in T cells, and published observations of other laboratories that B cells are not important in the early response to natural infection with *F. tularensis*[34].

DISCUSSION

Similarities in signaling pathways stemming from TLR and ER stress receptors have been noted[35]. Both IRE1α and TLRs trigger the production of ROS and acute phase proteins and both engage NEMO and TRAF adaptors to trigger inflammatory signaling components such as NF-κB and JNK[2, 36, 37]. These similarities suggest that these pathways may have co-evolved common strategies to respond to specific insults.

Our findings demonstrate that TLR and IRE1–XBP1 pathways are interconnected and cooperate to maximize innate immune responses to pathogens. We show that XBP1 mRNA is matured to its active form by TLR4 and TLR2, via a mechanism that requires the NADPH oxidase NOX2 in cooperation with TRAF6. Using NADPH oxidase inhibitors and NOX2-deficient macrophages we show that TLR activation of XBP1 requires ROS. Other pathways have been shown to trigger aspects of the ER-stress response in an ROS-dependent manner[24]. TNF treatment, for example, promotes PERK, ATF6α and IRE1 activation in a ROS-dependent fashion whereas ROS production by arsenite activates eIF2α phosphorylation but not PERK or IRE1α, indicating that different oxidative stresses selectively activate different downstream pathways[38]. In the case of TLRs we observe a non-traditional and specific activation of the IRE1-XBP1 pathway.

Surprisingly, the new function of the IRE1-XBP1 pathway in macrophages that we have uncovered here is ER-stress independent. We demonstrate that TLR4 and TLR2 stimulation triggered IRE1 phosphorylation and XBP1 mRNA maturation in the absence of any other ER-stress markers such as ATF6α processing, PERK phosphorylation or induction of ER-stress dependent genes encoding CHOP, BiP, ERdj4 and PDI. Consistent with a previous report describing that prolonged stimulation with low doses of LPS inhibits ER-stress mediated ATF4 activation and CHOP induction[39], we found similar inhibition in macrophages. Moreover, we observed that, in macrophages, ER-stress inhibition occurred very rapidly after activation of TLR2 and TLR4 and affected all the branches of the ER-stress response. ATF6α and PERK branches were inhibited as was expression of known XBP1-target genes such as *ERdj4*. These findings clearly demonstrate that TLR signaling broadly regulates ER-stress responses and provide some rationale for why TLR2 and TLR4 do not trigger known XBP1 and ER-stress dependent genes, despite IRE1 and XBP1 activation. Due to the complex and cooperative nature of the ER-stress response it is likely that deficiency in ATF6α and PERK activation contribute to the absence of genes normally induced by ER-stress. Having established that XBP1 activation downstream of TLR2 and

TLR4 does not contribute to an ER-stress response, we investigated the role of XBP1 in regulating TLR responses.

Certain transcription factors can modulate the amplitude and nature of innate immune responses via feedback loops that allow fine-tuning of transcriptional programs appropriate to a given host-pathogen interaction[5]. For example, ATF3 (ref. [6]) and IRF4 (refs. [40,41]), negatively regulate TLR4 signaling, while C/EBPδ. was identified as an amplifier of TLR induced signals[42]. Here we identify XBP1 as a regulatory factor that enhances cytokine production by TLR2 and TLR4. We provide several lines of evidence that XBP1 functions in a positive feedback loop to sustain TLR signaling in macrophages. First, TLR2 and TLR4 signaling from the plasma membrane activated IRE1α to promote XBP1 mRNA maturation and production of an active XBP1s protein.

Second, XBP1 deficiency in macrophages impaired sustained production of specific cytokines including IL-6 and IFN-β upon stimulation with TLR agonists or infection with the intracellular pathogen *F.tularensis* without affecting early production of these cytokines. Third, consistent with the hypothesis that XBP1 enhanced gene transcription, pharmacological activation of XBP1 synergistically augmented TLR production of IL-6. This finding is consistent with a report showing that a macrophage cell line RAW267.4 overexpressing XBP1s or stimulated with the ER-stress inducer, thapsigargin had increased IFN-β production upon stimulation with LPS[43]. Finally, we show in *in vivo* experiments in mice that XBP1 was important for early responses to aerosol infection with the human pathogen *F. tularensis*. Interestingly, XBP1 is critical for survival in *Caenorhabditis elegans* infected with pathogenic bacteria expressing pore-formin toxins, suggesting that its role in innate immunity has evolved through evolution[44].

We performed ChIP to show that XBP1 was recruited to the *Il6* and *Tnf* promoters. XBP1 *per se* was insufficient to trigger a substantial increase in IL-6 or TNF production, in ER-stressed macrophages. Indeed XBP1 activation synergized with TLR signaling to activate these promoters, suggesting that the mechanisms by which XBP1 regulates ER-stress responsive genes or the genes involved in the inflammatory response may differ. HAC1, the yeast XBP1 homologue, has been shown to regulate ER-stress responses by directly binding ER-stress responsive elements at the promoter of target genes. On the other hand, HAC1 has been shown to regulate early meiotic gene differentiation and responses to nitrogen starvation, indirectly by binding the histone deacetylase complex (HDAC)[45]. It is therefore possible that in mammals, XBP1 may also regulate non-ER-stress related gene expression by orchestrating chromatin modification or other transcriptional regulatory elements at specific promoters.

The finding that ER-stressed macrophages are hyperesponsive to TLR stimulation in an XBP1-dependent manner (as evidenced by the phenotype of XBP1-deficient macrophages), supports the notion that XBP1 is a positive regulator of TLR gene induction. It also supports the idea that ER-stress *per se* may promote inflammation by regulating the intensity and duration of innate responses. In line with this hypothesis, it has been shown that ER-stress caused by HLA-B27 misfolding enhances IL-23 production in a rat model of spondyloarthritis[46]. Because some diseases such as atherosclerosis, cystic fibrosis, inflammatory bowel disease and type 2 diabetes are characterized by features of both ER-stress and inflammation[47-49], it will be interesting to determine whether ER-stress (and XBP1 activation) is a major hallmark of tissue malfunction and damage contributing to chronic low-grade inflammation and hyper-inflammatory responses to inflammatory stimuli by further exacerbating TLR-driven responses. Moreover the development of pharmacological inhibitors of the IRE1-XBP1 pathway could present a new therapeutic

strategy aimed at reducing harmful TLR-mediated inflammation while activators of this pathway may enhance innate immunity in the setting of vaccination or natural infection.

Supplementary Material

Refer to Web version on PubMed Central for supplementary material.

Acknowledgments

We thank M. Greenblatt, M. Wein, V. Lazarevic and C.Hetz for thoughtful comments on the manuscript; D. Malhotra for assistance with the experiments in Figs 3&4; Alexandra Bolm for excellent technical assistance; G. Chu for analysis of the liver histology, V. Lazarevic, I. Kramnik and R. Pollack for help with the *F. tularensis* aerosol set-up, and S. Akira, P. Goldstein, J. Patterson, R. Medzhitov, K. Mori, J. Tschopp and the Broad Institute for generous provision of reagents. Supported by NIH grants AI32412 and AI56296, a grant from The Ragon Institute of MGH, MIT, Harvard (LHG) and grants from the American Heart Association (A-HL), the Leukemia and Lymphoma Society (XC) and the Human Frontier Science Program (FM).

Appendix

METHODS

Reagents

LPS, Pam_3CSK_4, the diacylated synthetic lipoprotein FSL1 and other TLR ligands were purchased from Invivogen. Muramyl dipeptide, tunicamycin, sulfasalazine, SB203580, SP600125 PD98059, tauroursodeoxycholic acid (TUDCA), diphenyleneiodonium chloride and apocynin were purchased from Calbiochem. 4-phenyl butyric acid (4-PBA) was obtained from Sigma–Aldrich.

Immunoblotting

Total cell extracts were loaded on SDS-PAGE for separation and transferred to PDVF membranes. IRE1α phosphorylation was monitored by phos-tag SDS-PAGE[19]. For immunoblot the following antibodies were used: anti-XBP1s (Poly6195; Biolegend), anti-phospho PERK (16F8), anti-total PERK (C33E10), IRE1α (14C10) and phospho-JNK (9251) (Cell Signaling), HSP90 (H114), IkappaBβ (C20) and CHOP (B3) (Santa Cruz Biotechnology), anti-ATF6α[50] and anti-pro-IL-1β[51] were gifts of K. Mori, Kyoto University, and J. Tschopp, University of Lausanne, respectively.

RNA extraction, RT-PCR and XBP1 splicing assay

Total RNA was prepared using Trizol (Invitrogen) and cDNA synthesis with High capacity cDNA Reverse transcription kit purchased from Applied Biosystems. Quantitative RT-PCR was performed employing SYBR green fluorescent reagent on a Mx3005P® QPCR System from Strategene. The relative amounts of mRNA were calculated from the values of comparative threshold cycle by using β-actin as control. Primer sequences were obtained from the Primer Data bank (http://pga.mgh.harvard.edu/primerbank/index.html). The following primers were used: for mIL-1β FW: 5′-CAACCAACAAGTGATATTCTCCATG-3′, RW 5′-GATCCACACTCTCCAGCTGCA-3′; mIL-6, FW 5′-GAGGATACCACTCCCAACAGACC-3′, RW 5′-AAGTGCATCATCGTTGTTCATACA-3′; mISG15, FW 5′-AGCGGAACAAGTCACGAAGAC-3′, RW 5′-TGGGGCTTTAGGCCATACTC-3′; mTNF, FW 5′-CATCTTCTCAAAATTCGAGTGACAA-3′, RW 5′-TGGGAGTAGACAAGGTACAACCC-3′; mActin, FW: 5′-TACCACCATGTACCCAGGCA-3′, RW 5′-CTCAGGAGGAGCAATGATCTTGAT-3′; Bip, FW 5′-TCATCGGACGCACTTGGA-3′, RW 5′-CAACCACCTTGAATGGCAAGA-3′

CHOP FW 5′-GTCCCTAGCTTGGCTGACAGA-3′ RW 5′-TGGAGAGCGAGGGCTTTG-3′; PDI, FW 5′-CAAGATCAAGCCCCACCTGAT-3′ RW 5′-AGTTCGCCCCAACCAGTACTT-3′; ERdj4, FW 5′-CCCCAGTGTCAAACTGTACCAG-3′ RW 5′-AGCGTTTCCAATTTTCCATAAATT-3′; WSF1, FW 5′-CCATCAACATGCTCCCGTTC-3′ RW 5′-GGGTAGGCCTCGCCAT-3′.

XBP1 splicing assay was performed as previously described [52]. In brief, PCR primers 5′-ACACGCTTGGGAATGGACAC-3′ and 5′-CCATGGGAAGATGTTCTGGG-3′ encompassing the spliced sequences in XBP1 mRNA were used for the PCR amplification, the PCR products subjected to electrophoresis on a 2.5% agarose gel and visualized by ethidium bromide staining.

ELISA

ELISA for mouse IL-6 was done by using 4 μg/ml of capture antibody (MP5-20F3; BD Biosciences), 2 μg/ml of biotinylated secondary antibody (MP5-32C11; BD Biosciences) and a 1:1000 dilution of alkaline phosphatase-conjugated streptavidin (Sigma).

Chromatin immunoprecipitations (ChIP)

ChIP assays were performed as described previously[53]. Cells were crosslinked with 1% formaldehyde for 10 min at room temperature, and formaldehyde was then inactivated by the addition of 125 mM glycine. Chromatin extracts containing DNA fragments with an average size of 500 bp were immunoprecipitated using anti-XBP1s or anti-GST (B-14, sc-138, Santa Cruz Biotechnology) antibody. All ChIP experiments were repeated at least three times. For all the primers used, each gave a single product of the right size, as confirmed by dissociation curve analysis. These primers also gave no DNA product in the no-template control. The primers used for real-time PCR to quantitate the ChIP-enriched DNA are as follows:

Il6 promoter

1. 5′-ACAGAGCCTACTTTCAGCCTGGAATCATT and 5′-ATGACAGGATTTGAATCTGAAGGTGGTACG;
2. 5′-TATTTCTGTACTTCACCCACTTTACCCAC and 5′-GCACCCAACCTGGACAACAGACAGTAATG;
3. 5′-CCTGCGTTTAAATAACATCAGCTTTAGCTT and 5′-GCACAATGTGACGTCGTTTAGCATCGAA;
4. 5′-GGAGCCCACCAAGAACGATAGTCAATTCCA and 5′-AAAACCGGCAAGTGAGCAGATAGCAC;
5. 5′-GCCTTCTTGGGACTGATGCTGGTGACAAC and 5′-GATTTCCCAGAGAACATGTGTAATTAAGCC;

Il1b promoter

1. 5′-CCTGGGCTCTCTGAGTTAGCAGTCTAGTGA and 5′-AGTGCAAAGGTGGTGAACGAGGCATCTG;
2. 5′-GGCTTGCTTCCAGAGTTCCCTGACCCTAT and 5′-GAGTTTGGTAACTGGATGGTGCTTCTGTGC;
3. 5′-GCCCATTTCCACCACGATGACACACT and 5′-TTTCCCTTGGGTTAACTGATTTCACAACAA;

4. 5′-CCACTGATGGACTTTGGGCTTTTTATTTAT and 5′-GGAAGGAAGCAACAGCAGAGCCAAACC;

***TNF* enhancer—**5′-GCCCTTCCTGAGAGTGGTTATAGACGATGC and 5′-GGTAAGCCTTGGCTAAGCTGTGTCACGG;

***TNF* promoter—**5′-CCAGCCAGCAGAAGCTCCCTCAGCGAG and 5′-GCGGATCATGCTTTCTGTGCTCATGGTGTC.

***Erdj4* promoter—**5′-AGTGACGCAAGGACCAAACG and 5′-CTACACGAAACGCTTCCCCA

***RANTES* promoter**

1. 5′-GGAAAAGCCTCCAGTGTCCAGCTGAGAT and 5′-CCAGGGAAAGGCACAACTTGTAAAACTGTT;
2. 5′-CTTGGGACCATATGAGCACATCAGTATGTT and 5′-GTCTGCAATTCTCTGGCTGTCAGTCCT;
3. 5′-CTCCCATTCCCCTCCACTGCATCCATGTTC and 5′-TAGCATTCAATCAGTCTCCGCCTTAT;
4. 5′-CCACAGAGATTCTTTGTAGCCCTATCAGA and 5′-GAGATTTGTTGTAAGGAATTTGCCAGGTAA;
5. 5′-TTAAGACAACAGCTCCCTGCTACCTG and 5′-AAACTGAAATCACCCTTGGAAGTATGACTC;
6. 5′-GGGTGATTTCAGTTTTCTTTTCCATTTTG and 5′-CTGTGGGAGATGCATGTGCTGTCTCAGAGT

***Apoa4* promoter (control)—**5′-CTGTGTGCTGTCAGCTTCCAC and 5′-CCTCCTCCCCAGTGTGACTC

Knockdown of IRE1α, BI-1, TRAF6 and NEMO

We generated stable J744 macrophage populations by targeting *IRE1α*, , *BI-1, TRAF6* and *NEMO* mRNA by using the lentiviral delivery of specific shRNAs followed by puromycin (4 μg/ml) selection. shRNA targeting *luciferase* mRNA were used as a control. Constructs were generated by The Broad Institute (Boston, USA). For every gene five different targeting constructs were screened and the most efficients were selected. Optimal targeting sequences identified for mouse *IRE1α*, *TRAF6, NEMO* and *BI-1* are 5′-GCTCGTGAATTGATAGAGAAA; 5′-CCCAGGCTGTTCATAATGTTA and 5′-AGACTACGACAGCCACATTAA, 5′-CCTCTTTGATACTCAGCTCAT respectively.

Knockdown efficiency was tested by immunoblot for IRE1α and by real-time PCR for TRAF6, NEMO and BI-1 as shown in Supplementary Fig. 9.

Transduction of J774 cells with active IRE1α

J774 macrophages were transduced as described [54]. Briefly the cells were incubated for 1 h with 6 μg/ml of endo-porter (GeneTools) and various amounts of an active recombinant IRE1α fragment spanning mainly the kinase and ribonuclease domains of IRE1α[26] (gift from John Patterson, MannKind Corp).

Viability assay

Cell viability was determined using the MTT [3-(4,5-dimethylthiazol-2-yl)-2,5-diphenyl tetrazolium bromide]-based assay, Cell Titer 96 Non Radioactive viability assay as instructed by the manufacturer (Promega).

Mice

Mice were housed in the pathogen-free facility at the Harvard School of Public Health and were handled in accordance with guidelines from the Center for Animal Resources and Comparative Medicine at Harvard Medical School. Protocol numbers: 1009-R98, 04567, 03743. MyD88 deficient mice on a C57BL/6 background were a gift from P. Goldstein and S. Akira. TIRAP knockout mice were a gift from R. Medzhitov, Yale University. C3H/HeOuJ, C3H/HeJ, Lps2 (TRIF also known as TICAM1 deficient), TLR2 and NOX2 deficient mice (*Cybb*$^{-/-}$) were purchased from Jackson Laboratories. Mice lacking XBP1 in hematopoietic cells including macrophages were generated from mating Xbp1^{flox} mice harboring *lox*P sites in the first and second intron of the *Xbp1* gene to mice expressing an interferon-dependent Cre recombinase as previously described[25]. Five week old mice were intraperitoneally injected 1 or 3 times with 250 μg of poly(I:C) at 2 day intervals to induce Cre expression and used for experiments 2-3 weeks to several months after the final poly(I:C) injection. Sex-matched Xbp1^{flox} littermates injected with poly(I:C) were used as WT controls throughout the study.

Bone marrow-derived macrophages (BMMs)

Bone marrow was collected from femurs in DMEM/F12 medium supplemented with 10% L-929 cell-conditioned media, 10% heat inactivated FCS and 1 ng/ml IL-3 (PreproTech) and antibiotics. After two days culture non-adherent precursors were plated in 12 wells plate at 2 × 10^5 cells/well in DMEM/F12 medium supplemented with 10% L-929 cells conditioned media, 10% heat inactivated FCS and antibiotics for 6 to 10 days. The media was changed every other day. Except for Francisella infection, all experiments involving stimulation kinetics were performed to harvest all samples simultaneously.

Human monocyte-derived macrophage culture

Peripheral blood mononuclear cells (PBMCs) were isolated from freshly drawn blood of healthy donors by Ficoll-Paque gradient centrifugation (GE healthcare). CD14+ monocytes were isolated from PBMC by positive selection using CD14 magnetic beads (Miltenyi Biotec). Monocyte-derived macrophages were obtained following 7 days of culture in Macrophage serum free medium (Invitrogen) supplemented with 10% human serum (Sigma), 50 ng/ml human MCSF (R&D) and 100U/ml penicillin and 0.1 mg/ml streptomycin. Human samples from anonymous donors were collected with informed consent in accordance to guidelines from the Harvard and Dana Farber Cancer institute office for the protection of research subjects. Protocol number DFCI 01-206.

F. tularensis LVS infection

F. tularensis subsp. holarctica Live Vaccine Strain (LVS) was obtained from the New England Regional Center of Excellence/Biodefense and Emerging Infectious Diseases (Boston, Massachusetts). LVS was grown in modified Mueller-Hinton broth, harvested and frozen at −80°C in 1 ml aliquots (10^{10} CFU/ml). For infection 1 ml LVS stock is grown in 25 ml of Mueller-Hinton broth at 37°C, with shaking overnight to OD600 of 0.3-0.4 Antibiotic-free macrophages were infected with *F. tularensis* LVS at a multiplicity of infection (MOI) of 10:1 (bacterium-to-macrophage). 2 h after infection, the cell monolayer was washed three times with sterile PBS and incubated for 45 min with media containing 50 μg/ml gentamicin to eliminate extracellular bacteria. Macrophages were then washed three

times with PBS and gentamicin-free media and analyzed as described. For aerosol infection, 1 ml LVS stock was grown in 25 ml of Mueller-Hinton broth at 37 °C, with shaking overnight. The inoculation stock is diluted to 7×10^7 CFU/ml in sterile PBS containing 20% glycerol. LVS aerosols are generated with a Lovelace nebulizer using a commercial nose-only exposure apparatus (InTox Products). In each experiment, mice were exposed to LVS containing aerosols for 30 min, followed by 10 min of clean air, where aerosols are delivered to the exposure ports at a flow rate of 6 l/min. Seven days after aerosol infection, lungs, liver and spleen from infected mice were homogenized in 10 ml of sterile PBS and the suspension plated on Mueller-Hinton plates to determine the bacterial burden.

Statistic analysis

Significant differences between treatment groups were identified with a *t*-test. *P* values of less than 0.05 were considered statistically significant.

REFERENCES IN METHODS

19. Sha H, et al. The IRE1alpha-XBP1 pathway of the unfolded protein response is required for adipogenesis. Cell Metab. 2009; 9:556–564. [PubMed: 19490910]
26. Lisbona F, et al. BAX inhibitor-1 is a negative regulator of the ER stress sensor IRE1alpha. Mol Cell. 2009; 33:679–691. [PubMed: 19328063]
50. Yamamoto K, et al. Transcriptional induction of mammalian ER quality control proteins is mediated by single or combined action of ATF6alpha and XBP1. Dev Cell. 2007; 13:365–376. [PubMed: 17765680]
51. Martinon F, Pétrilli V, Mayor A, Tardivel A, Tschopp J. Gout-associated uric acid crystals activate the NALP3 inflammasome. Nature. 2006; 440:237–241. [PubMed: 16407889]
52. Iwakoshi NN, et al. Plasma cell differentiation and the unfolded protein response intersect at the transcription factor XBP-1. Nat Immunol. 2003; 4:321–329. [PubMed: 12612580]
53. Bhoj VG, Chen ZJ. Linking retroelements to autoimmunity. Cell. 2008; 134:569–571. [PubMed: 18724930]
54. Summerton JE. Endo-Porter: A Novel Reagent for Safe, Effective Delivery of Substances into Cells. Ann N Y Acad Sci. 2005; 1058:62–75. [PubMed: 16394126]

REFERENCES

1. Janeway CA, Medzhitov R. Innate immune recognition. Annu. Rev. Immunol. 2002; 20:197–216. [PubMed: 11861602]
2. Kawai T, Akira S. TLR signaling. Semin Immunol. 2007; 19:24–32. [PubMed: 17275323]
3. O'Neill LAJ, Bowie AG. The family of five: TIR-domain-containing adaptors in Toll-like receptor signalling. Nat Rev Immunol. 2007; 7:353–364. [PubMed: 17457343]
4. Ravasi T, Wells CA, Hume DA. Systems biology of transcription control in macrophages. Bioessays. 2007; 29:1215–1226. [PubMed: 18008376]
5. Roach JC, et al. Transcription factor expression in lipopolysaccharide-activated peripheral-blood-derived mononuclear cells. Proc Natl Acad Sci USA. 2007; 104:16245–16250. [PubMed: 17913878]
6. Gilchrist M, et al. Systems biology approaches identify ATF3 as a negative regulator of Toll-like receptor 4. Nature. 2006; 441:173–178. [PubMed: 16688168]
7. Kono H, Rock KL. How dying cells alert the immune system to danger. Nat Rev Immunol. 2008; 8:279–289. [PubMed: 18340345]
8. Medzhitov R. Origin and physiological roles of inflammation. Nature. 2008; 454:428–435. [PubMed: 18650913]
9. Sansonetti PJ. The innate signaling of dangers and the dangers of innate signaling. Nat Immunol. 2006; 7:1237–1242. [PubMed: 17110939]

10. Ron D, Walter P. Signal integration in the endoplasmic reticulum unfolded protein response. Nat Rev Mol Cell Biol. 2007; 8:519–529. [PubMed: 17565364]
11. Lin JH, et al. IRE1 signaling affects cell fate during the unfolded protein response. Science. 2007; 318:944–949. [PubMed: 17991856]
12. Nau GJ, et al. Human macrophage activation programs induced by bacterial pathogens. Proc Natl Acad Sci USA. 2002; 99:1503–1508. [PubMed: 11805289]
13. Blumenthal A, et al. Common and unique gene expression signatures of human macrophages in response to four strains of Mycobacterium avium that differ in their growth and persistence characteristics. Infect Immun. 2005; 73:3330–3341. [PubMed: 15908359]
14. Schurr JR, et al. Central role of toll-like receptor 4 signaling and host defense in experimental pneumonia caused by Gram-negative bacteria. Infect Immun. 2005; 73:532–545. [PubMed: 15618193]
15. Goodall JC, Ellis L, Yeo GSH, Gaston JSH. Does HLA-B27 influence the monocyte inflammatory response to lipopolysaccharide? Rheumatology (Oxford). 2007; 46:232–237. [PubMed: 16877465]
16. Endo M, Oyadomari S, Suga M, Mori M, Gotoh T. The ER stress pathway involving CHOP is activated in the lungs of LPS-treated mice. Journal of Biochemistry. 2005; 138:501–507. [PubMed: 16272146]
17. Zhang K, et al. Endoplasmic reticulum stress activates cleavage of CREBH to induce a systemic inflammatory response. Cell. 2006; 124:587–599. [PubMed: 16469704]
18. Ishiai M, et al. FANCI phosphorylation functions as a molecular switch to turn on the Fanconi anemia pathway. Nat Struct Mol Biol. 2008; 15:1138–1146. [PubMed: 18931676]
20. Matsuzawa A, et al. ROS-dependent activation of the TRAF6-ASK1-p38 pathway is selectively required for TLR4-mediated innate immunity. Nat Immunol. 2005; 6:587–592. [PubMed: 15864310]
21. Takeshita F, et al. TRAF4 acts as a silencer in TLR-mediated signaling through the association with TRAF6 and TRIF. Eur. J. Immunol. 2005; 35:2477–2485. [PubMed: 16052631]
22. Ha YJ, Lee JR. Role of TNF receptor-associated factor 3 in the CD40 signaling by production of reactive oxygen species through association with p40phox, a cytosolic subunit of nicotinamide adenine dinucleotide phosphate oxidase. J Immunol. 2004; 172:231–239. [PubMed: 14688330]
23. Grandvaux N, Soucy-Faulkner A, Fink K. Innate host defense: Nox and Duox on phox's tail. Biochimie. 2007; 89:1113–1122. [PubMed: 17537563]
24. Malhotra JD, Kaufman RJ. Endoplasmic reticulum stress and oxidative stress: a vicious cycle or a double-edged sword? Antioxid Redox Signal. 2007; 9:2277–2293. [PubMed: 17979528]
25. Lee A-H, Scapa E, Cohen D, Glimcher L. Regulation of Hepatic Lipogenesis by the Transcription Factor XBP1. Science. 2008; 320:1492. [PubMed: 18556558]
27. Rick Lyons C, Wu TH. Animal models of Francisella tularensis infection. Ann N Y Acad Sci. 2007; 1105:238–265. [PubMed: 17395735]
28. Cole LE, et al. Immunologic consequences of Francisella tularensis live vaccine strain infection: role of the innate immune response in infection and immunity. J Immunol. 2006; 176:6888–6899. [PubMed: 16709849]
29. Katz J, Zhang P, Martin M, Vogel SN, Michalek SM. Toll-like receptor 2 is required for inflammatory responses to Francisella tularensis LVS. Infect Immun. 2006; 74:2809–2816. [PubMed: 16622218]
30. Cole, et al. TLR2-Mediated Signaling Requirements for Francisella tularensis LVS Infection of Murine Macrophages. Infect Immun. 2007
31. Elkins KL, Cowley SC, Bosio CM. Innate and adaptive immunity to Francisella. Ann N Y Acad Sci. 2007; 1105:284–324. [PubMed: 17468235]
32. Malik M, et al. Toll-like receptor 2 is required for control of pulmonary infection with Francisella tularensis. Infect Immun. 2006; 74:3657–3662. [PubMed: 16714598]
33. Abplanalp AL, Morris IR, Parida BK, Teale JM, Berton MT. TLR-dependent control of Francisella tularensis infection and host inflammatory responses. PLoS ONE. 2009; 4:e7920. [PubMed: 19936231]

34. Elkins KL, Bosio CM, Rhinehart-Jones TR. Importance of B cells, but not specific antibodies, in primary and secondary protective immunity to the intracellular bacterium Francisella tularensis live vaccine strain. Infect Immun. 1999; 67:6002–6007. [PubMed: 10531260]
35. Zhang K, Kaufman RJ. From endoplasmic-reticulum stress to the inflammatory response. Nature. 2008; 454:455–462. [PubMed: 18650916]
36. Hu P, Han Z, Couvillon AD, Kaufman RJ, Exton JH. Autocrine tumor necrosis factor alpha links endoplasmic reticulum stress to the membrane death receptor pathway through IRE1alpha-mediated NF-kappaB activation and down-regulation of TRAF2 expression. Mol Cell Biol. 2006; 26:3071–3084. [PubMed: 16581782]
37. Urano F, et al. Coupling of stress in the ER to activation of JNK protein kinases by transmembrane protein kinase IRE1. Science. 2000; 287:664–666. [PubMed: 10650002]
38. Xue X, et al. Tumor necrosis factor alpha (TNFalpha) induces the unfolded protein response (UPR) in a reactive oxygen species (ROS)-dependent fashion, and the UPR counteracts ROS accumulation by TNFalpha. J Biol Chem. 2005; 280:33917–33925. [PubMed: 16107336]
39. Woo CW, et al. Adaptive suppression of the ATF4-CHOP branch of the unfolded protein response by toll-like receptor signalling. Nat Cell Biol. 2009; 11:1473–1480. [PubMed: 19855386]
40. Negishi H, et al. Negative regulation of Toll-like-receptor signaling by IRF-4. Proc Natl Acad Sci USA. 2005; 102:15989–15994. [PubMed: 16236719]
41. Honma K, et al. Interferon regulatory factor 4 negatively regulates the production of proinflammatory cytokines by macrophages in response to LPS. Proc Natl Acad Sci USA. 2005; 102:16001–16006. [PubMed: 16243976]
42. Litvak V, et al. Function of C/EBPdelta in a regulatory circuit that discriminates between transient and persistent TLR4-induced signals. Nat Immunol. 2009
43. Smith JA, et al. Endoplasmic reticulum stress and the unfolded protein response are linked to synergistic IFN-beta induction via X-box binding protein 1. Eur. J. Immunol. 2008; 38:1194–1203. [PubMed: 18412159]
44. Bischof LJ, et al. Activation of the unfolded protein response is required for defenses against bacterial pore-forming toxin in vivo. PLoS Pathog. 2008; 4:e1000176. [PubMed: 18846208]
45. Schröder M, Clark R, Liu CY, Kaufman RJ. The unfolded protein response represses differentiation through the RPD3-SIN3 histone deacetylase. EMBO J. 2004; 23:2281–2292. [PubMed: 15141165]
46. Delay ML, et al. HLA-B27 misfolding and the unfolded protein response augment interleukin-23 production and are associated with Th17 activation in transgenic rats. Arthritis Rheum. 2009; 60:2633–2643. [PubMed: 19714651]
47. Lin, Walter, Yen. Endoplasmic Reticulum Stress in Disease Pathogenesis. Annu Rev Pathol. 2007
48. Kaser A, et al. XBP1 links ER stress to intestinal inflammation and confers genetic risk for human inflammatory bowel disease. Cell. 2008; 134:743–756. [PubMed: 18775308]
49. Ozcan U, et al. Endoplasmic reticulum stress links obesity, insulin action, and type 2 diabetes. Science. 2004; 306:457–461. [PubMed: 15486293]

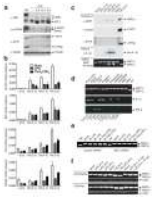

Figure 1. TLRs activate XBP1 mRNA maturation in the absence of ER-stress

(**a**), IRE1α activation (phos-tag SDS-PAGE), PERK phosphorylation and ATF6α processing in LPS or tunicamycin (TM) stimulated J774 cells extracts. (**b**), Induction of CHOP, BiP, PDI and Erdj4 mRNA was measured in untreated (6h), TM-treated (2, 4 and 6 h), TM plus LPS (grey bars), or Pam_3CSK_4 (black bars) treated J774 cells by real-time PCR relative to β-actin (mean and s.e.m. of triplicates). J774 cells were also left untreated (white bars). (**c**), Immunoblot of XBP1s, CHOP and processed ATF6α in nuclear extracts (Nuclear xt) of J774 macrophages stimulated with LPS or TM for the indicated times. Pro-IL-1β levels in total extracts (Total xt) is shown. XBP1 mRNA maturation was analyzed by RT-PCR (bottom). (**d**), The ability of muramyl dipeptide (MDP) and a panel of specific TLRs agonists to promote XBP1 activation with TM as a positive control was tested. XBP1 splicing and control genes IL-1β and IFN-β were monitored by RT-PCR. (**e**), XBP1 splicing by RT-PCR in LPS, Pam_3CSK_4 or TM treated J774 cells stably transduced with IRE1α or control shRNA lentiviruses. (**f**) XBP1 mRNA maturation was analyzed by RT-PCR in bone marrow derived macrophages (BMMs) from TLR4 competent (C3H/HeOuJ) or defective (C3H/HeJ) mice stimulated with LPS 100 ng/ml or 10 μg/ml TM (time and dose dependent concentrations of LPS indicated above lanes)., XBP1u, unspliced XBP1; XBP1s, spliced (mature) XBP1; p-IRE1, p-PERK, phosphorylated IRE1 and PERK respectively; ATF6p, processed form of ATF6α. Data are representative of at least three independent experiments.

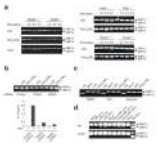

Figure 2. XBP1 activation requires proximal TLR signaling

(**a**) BMMs from MyD88, TIRAP, TRIF (*Ticam1*) deficient mice or littermate controls, were stimulated with 100 ng/ml of the TLR4 agonist LPS, the TLR1/2 agonist Pam_3CSK_4, the TLR6/2 agonist FSL1 or 10 μg/ml TM as indicated. XBP1 mRNA maturation was analyzed by RT-PCR. (**b,c**) J774 cells stably transduced with lentivirus encoding TRAF6, and NEMO specific shRNA or a control shRNA (**b**), or pretreated for 5 min with NADPH oxidase inhibitors diphenyleneiodonium chloride (DPI, 10 μM), apocynin (1 mM) or the carrier DMSO (1 μl/ml) (**c**), were stimulated with LPS, Pam_3CSK_4 or TM as indicated and analyzed for XBP1 mRNA splicing by RT-PCR. To confirm knockdown efficiency, IL-6 production upon stimulation with LPS was measured by ELISA (**b**, bottom). (**d**), WT or NOX2-deficient macrophages (*Cybb* $^{-/-}$) were stimulated as indicated and monitored for XBP1 activation. Data are representative of three independent experiments.

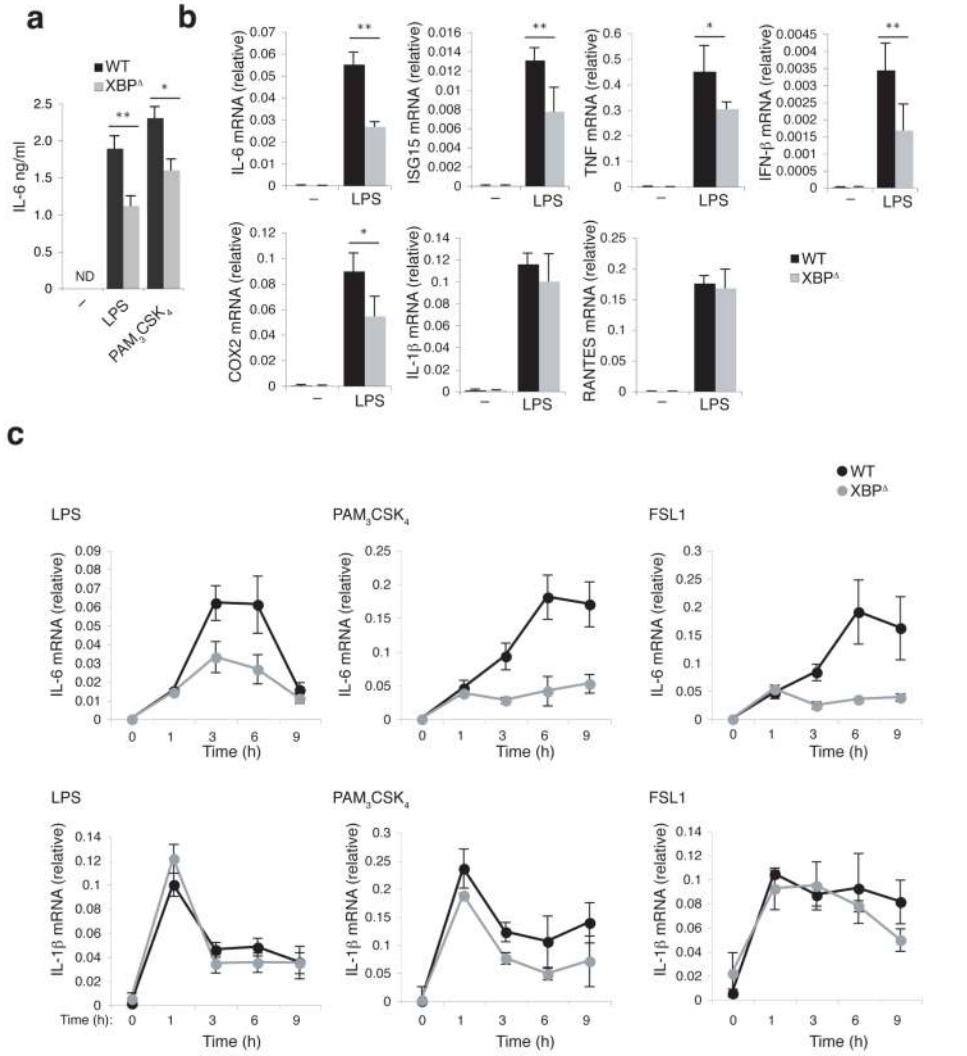

Figure 3. XBP1 is required for optimal TLR responses

(**a-c**) BMMs from XBP1 deficient (XBP1$^{\Delta}$) or littermate (WT) mice were stimulated with LPS, Pam_3CSK_4, or FSL1 as indicated. Supernatants were collected and analyzed for the production of IL-6 (**a**). mRNA was harvested and analyzed by real-time PCR to quantify cytokines (**b,c**). A time course is shown in **c** and 6 h stimulation time points are shown in **a** and **b**. Relative expression to β-actin is given. Data are from one representative of four (**a**) or three (**b, c**) independent experiments (mean and s.e.m). ** $P \leq 0.01$; * $P < 0.02$. ND, not detected.

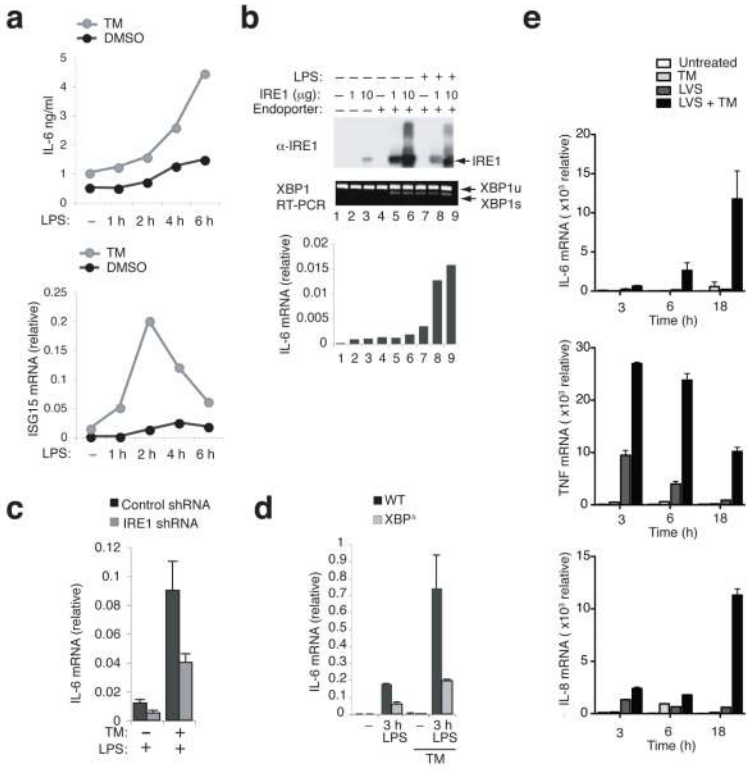

Fig. 4. IRE1α activation synergizes with TLRs to augment cytokine production

(**a**), Synergy for IL-6 production (ELISA) and ISG15 (RT-PCR) in J774 cells treated with carrier DMSO (black line) or 1 μg/ml TM (grey line) for 6 h in the presence or absence of LPS. Relative expression to β-actin is given. (**b**), J774 cells transduced with 1 or 10 μg of recombinant active IRE1α protein in the presence of endoporter (endo) for 1 h were stimulated with LPS for 6 h as indicated. Protein internalization and aggregation was monitored by immunoblot and *Il6* mRNA production by quantitative RT-PCR. Relative expression to β-actin is given. (**c**), J774 cells stably transduced with IRE1α or control shRNA lentiviruses were stimulated with LPS for 6 h and TM as indicated. IL-6 mRNA was monitored by RT-PCR. Relative expression to β-actin is given. (**d**), $XBP1^{\Delta}$ or littermate (WT) BMM untreated or prestimulated for 16 h with 100 ng/ml TM and then incubated with LPS for 3 h in fresh medium. IL-6 production was monitored by RT PCR. (**e**) Cytokine production (RT-PCR) in human macrophages untreated (white bars) or treated with TM (light grey bars), infected with *F. tularensis* live vaccine strain (LVS) (grey bars) or infected with LVS in the presence of TM (black bars) for 3 h, 6 h and 18 h as indicated. Relative expression to untreated samples is given. Results are representative of at least two independent experiments (mean and s.d. of triplicate assays (**c,d**) or duplicate assays (**e**)).

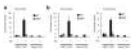

Figure 5. XBP1 recruitment to *Il6* and *Tnf* promoters

(**a,b**) ChIP analysis of XBP1 occupancy at the *Il6* promoter in unstimulated or TM-stimulated macrophages derived from littermate (WT) or XBP1$^{\Delta}$ mice. ChIP assay using GST antibody was performed as negative control (Mock ChIP). Fold enrichment is the relative abundance of DNA fragments at the *Il6* promoter (**a**) or at the *Tnf* promoter and enhancer (**b**) over a control region in the *Apoa4* promoter as quantified by real-time PCR. Data are representative of three independent experiments, (mean and s.d) of triplicates).

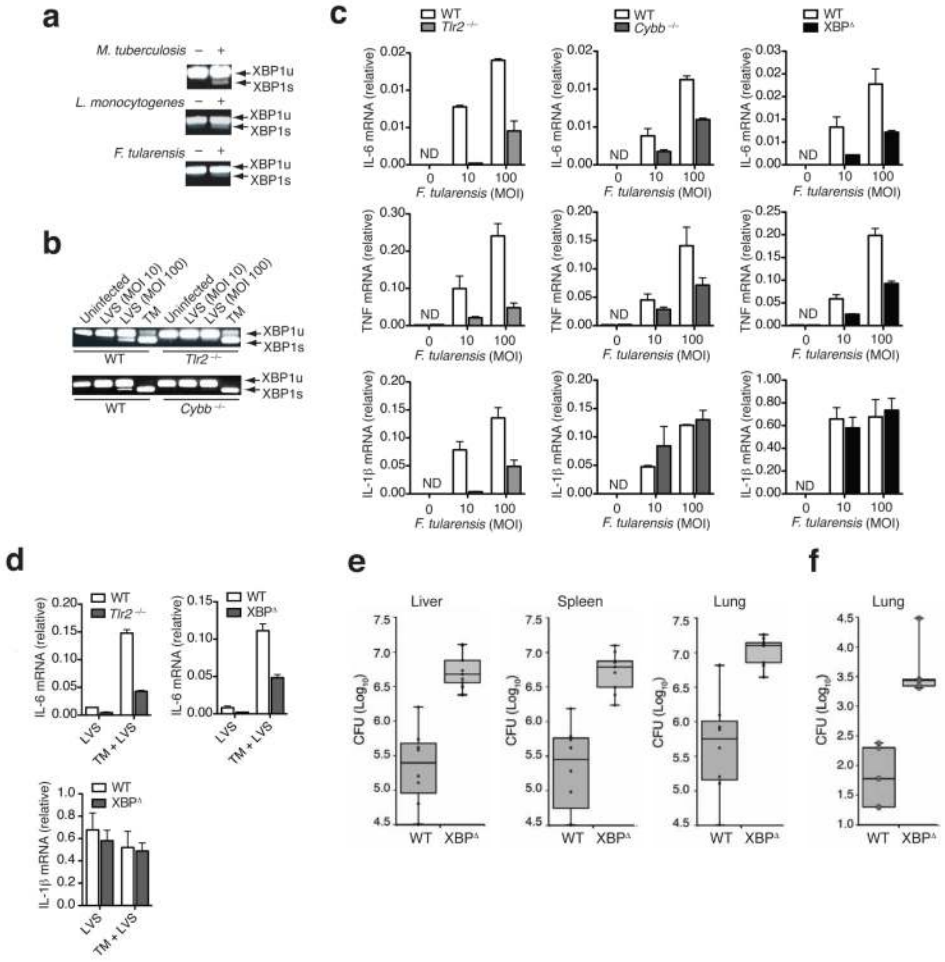

Figure 6. XBP1 deficiency impairs resistance to *F.tularensis* LVS infection

(**a**) BMM were left untreated (−) or infected at MOI 1:10 with *M. tuberculosis* for 6 h, *L. monocytogenes* for 8 h or *F.tularensis* for 24 h as indicated. XBP1s was monitored by RT-PCR. (**b**) BMMs of *Tlr2*$^{-/-}$, *Cybb*$^{-/-}$ and respective control mice were infected with *F.tularensis* at MOI 10:1, or MOI 100:1 for 8 h and analyzed for XBP1 splicing by RT-PCR. (**c**) BMMs from *Tlr2*$^{-/-}$, *Cybb*$^{-/-}$, XBP1$^{\Delta}$, or littermate (WT) mice were infected with *F. tularensis* LVS at an MOI of 10:1. 8 h post-infection, IL-6, TNF and IL-1β production was analyzed by real-time PCR. (**d**) BMMs from *Tlr2*$^{-/-}$, XBP1$^{\Delta}$ or littermate (WT) mice were infected with *F. tularensis* LVS at an MOI of 10:1 for 8 h in the presence or absence of TM. Cytokine production was measured by real-time PCR. (**e,f**), XBP1$^{\Delta}$ or littermate (WT) mice were infected via the aerosol route. Nine mice per group (**e**) were monitored for bacterial counts in the indicated organs (CFU) 7 days post infection. Five mice per group (**f**) were monitored 14 days post infection. Data are represented with Box and Whiskers extended to extreme data points, $P < 0.001$. Data are representative of three independent experiments (**a**, **c**) and two independent experiments (**b**, **d**) (mean and s.e.m of triplicates (**c**, **d**).